



# Probing amylin fibrillation at an early stage *via* a tetracysteine-recognising fluorophore



Shih-Ting Wang, Yiyang Lin, Chia-Chen Hsu, Nadav Amdursky, Christopher D. Spicer, Molly M. Stevens\*

Department of Materials, Department of Bioengineering and Institute for Biomedical Engineering, Imperial College London, Exhibition Road, London SW7 2AZ, United Kingdom

## ARTICLE INFO

### Keywords:

Amylin  
FAsH  
Fibrillation  
Early detection  
Amyloid inhibitor  
Glycosaminoglycan

## ABSTRACT

Amyloid fibrillation is a nucleation-dependent process known to be involved in the development of more than 20 progressive and chronic diseases. The detection of amyloid formation at the nucleation stage can greatly advance early diagnoses and treatment of diseases. In this work, we developed a new assay for the early detection of amylin fibrillation using the biarsenical dye 4,5-bis(1,3,2-dithiarsolan-2-yl)fluorescein (FAsH), which could recognise tetracysteine motifs and transform from non-fluorescent form into strongly fluorescent complexes. Due to the close proximity of two cysteine residues within the hydrophilic domain of amylin, a non-contiguous tetracysteine motif can form upon amylin dimerisation or oligomerisation, which can be recognised by FAsH and emit strong fluorescence. This enables us to report the nucleation-growth process of amylin without modification of the protein sequence. We showed that the use of this assay not only allowed the tracking of initial nucleation events, but also enabled imaging of amyloid fibrils and investigation of the effects of amyloid inhibitor/modulator toward amylin fibrillation.

## 1. Introduction

Type II diabetes (T2D) is an epidemic disease that leads to  $\beta$ -cell failure and many chronic macro- and microvascular complications [1]. One of the causes has been found to involve the fibrillation of amylin (or islet amyloid polypeptide, IAPP), which is co-secreted with insulin [2]. Amylin is a 37-amino acid peptide hormone, which possesses a disulphide bond between the cysteine residues Cys 2 and Cys 7 at the N-terminal domain (amylin residues 1–19), and carries three positive charges throughout the structure that stabilise the protein structure and give bioactivity. The over-production of amylin associated with insulin resistance and hyperinsulinemia in T2D triggers a nucleation-dependent self-assembly of amylin into intracellular or extracellular amyloid deposits, which is modulated by the core amyloidogenic sequence at the C-terminal domain (amylin residues 20–29). The self-assembly of amyloid proteins into fibrils is reported to undergo a nucleated polymerisation process via a two-step kinetic process. Fibril growth is triggered upon formation of a “critical nucleus” of amyloid aggregates in the early nucleation process, in which a large mass percentage of the small protein aggregates are converted into fibrils at an exponential rate. These amyloid aggregates (*i.e.* oligomers) formed at the early stage have been considered as the major cytotoxic species

[3–5]. It is therefore important to be able to detect these early aggregation species in order to prevent subsequent amyloid-induced pathology.

Amyloid oligomers have been reported in different sizes and shapes, including dimers, tetramers, hexamers and dodecamers [6–15]. However, few methods are able to detect and quantify the extent of oligomer formation and whether such species will subsequently lead to the formation of amyloid fibrils. Fluorescence has been the most commonly used technique to study the fibrillation of amyloid proteins. Several amyloid-reporting dyes such as Thioflavin-T (ThT), Congo red, Nile Red and 8-anilino-1-naphthalenesulphonic acid could indicate the formation of  $\beta$ -sheets or hydrophobic domains during amyloid fibrillation [8,16–19]. However, such fluorescent dyes targeting the core  $\beta$ -sheet region, only show increased fluorescence when a critical amount of fibril nucleus is formed, making them relatively insensitive to the formation of oligomers. In particular, ThT is widely exploited in detecting large fibrillar aggregates both *in vitro* and *in vivo* since it selectively binds to amyloid fibrils and emits bright fluorescence upon binding. However, the ThT assay is not suitable for monitoring the early aggregation events, as it does not bind to amyloid oligomers. New methods using two individual components of fluorescent protein fragments via bimolecular fluorescence complementation [20], FRET [21] and aggregation-induced emission [22], have been

\* Corresponding author.

E-mail address: [m.stevens@imperial.ac.uk](mailto:m.stevens@imperial.ac.uk) (M.M. Stevens).

developed for early detection of amyloid fibrillation. Recently, a MRI (magnetic resonance imaging) probe that pairs a magnetic nanostructure with an antibody has also been reported to detect the amyloid  $\beta$  oligomers in the brain that are responsible for the onset of disease [23].

In the work presented here, we have developed a new strategy to detect the early stages of amylin fibrillation in its native sequence, by using the protein sequence-selective biarsenical dye, 4,5-bis(1,3,2-dithiarsolan-2-yl)fluorescein (FLAsH), which exhibits increased fluorescence upon reacting with oriented tetracysteine motifs. The fluorogenic nature of the dye is based on an efficient thiol-arsenic ligand exchange reaction that converts the non-fluorescent 1,2-ethanedithiol (EDT)-bound form of FLAsH into strongly fluorescent complexes [24]. FLAsH has been shown to efficiently recognise the amino acid sequence, CCXXCC (where X represents any amino acids other than cysteine) allowing its use for imaging cells and studying protein-protein interactions [25,26]. FLAsH can also recognise two proximal bicysteine motifs (Cys-Cys) on separate strands when held in the correct orientation, allowing it to be used as a reporter for protein folding [24,25]. Recent work by Lee et al. has demonstrated the use of FLAsH to record the aggregation process of amyloid- $\beta$  (A $\beta$ ), by modifying the natural protein sequence with two consecutive cysteines, which subsequently become proximal ( $\sim 7$  Å) in the assembled state [27]. However, importantly this approach requires covalent conjugation of two cysteines which alters the native form of the amyloid protein. In this work, we demonstrate that FLAsH can be used to monitor the fibrillation of amylin, without needing to attach additional amino acids. Since amylin possesses two cysteines (Cys2 and Cys7) at the N-terminal domain, the aggregation of two or more amylin molecules will generate tetracysteine moieties that can be recognised by FLAsH. Particularly, the inter-strand proximity of amylin was reported to be  $\sim 4.7$  Å corresponding to the hydrogen bond spacing of two  $\beta$ -strand layers in the fibrillar state [28]. This allows the proximal orientation of four cysteines and effective binding of FLAsH to amylin. In principle, this method could be utilised to monitor the formation of amylin oligomers or even dimers. By taking advantage of the enhanced FLAsH fluorescence, this assay was also applied to image amylin fibrils with fluorescence microscopy. Furthermore, FLAsH was used as a probe to investigate the extent of amylin fibrillation in the presence of small-molecule inhibitor and glycosaminoglycan (GAG)-based modulators. Beyond the early detection study of amyloid fibrillation, we anticipate this assay can be applied in the field of high-throughput screening of amyloid inhibitors.

## 2. Materials and methods

### 2.1. Materials

Human amylin was purchased from Bachem. FLAsH and all the other chemicals were purchased from Sigma-Aldrich (U.K.). Milli-Q water (18 M $\Omega$ ) was used for the experiments.

### 2.2. Pre-treatment of amylin

To remove pre-existing aggregation structures, amylin powder was dissolved in hexafluoro-2-propanol (HFIP) in a sealed vial for 8 h at room temperature. After evaporating the solvent with N<sub>2</sub> gas, the pre-treated amylin powder was stored at  $-20$  °C.

### 2.3. Transmission electron microscopy (TEM) imaging

Amylin fibrils for TEM imaging were prepared by ageing amylin in 20 mM phosphate buffer (pH 7.5) for at least 2 days at room temperature. The sample was deposited on carbon film supported TEM grids and stained with 1 wt% uranyl acetate prior to imaging. TEM imaging was performed on a JEOL 2100F microscope with an acceleration voltage of 200 kV.

### 2.4. Atomic force microscopy (AFM) imaging

Amylin fibrils for AFM imaging were prepared by ageing amylin in 20 mM phosphate buffer (pH 7.5) for at least 2 days at room temperature. The sample was drop-cast on an oxygen plasma treated silicon wafer and left to dry in air prior to imaging. AFM imaging was performed on an AFM 5500 Microscope (Keysight Technologies, previously Agilent) in tapping mode in air. A HQ: NSC15/Al BS tip ( $\mu$ masch) was used for the topography imaging (tip radius of 8 nm, resonance frequency of 325 kHz, force constant of 40 N m<sup>-1</sup>).

### 2.5. Circular dichroism (CD)

The secondary structures of amylin monomer and fibrils were recorded by Jasco-715 circular dichroism spectrometer. The pre-formed fibrils were prepared by incubating amylin powder with 20 mM phosphate buffer (pH 7.5) for 24 h at room temperature. The samples were loaded in a quartz cell with an optical path length of 1.0 mm. The scanning speed was 50 nm/min, the data pitch was 0.1 nm, the response time was 4 s, and the band width was 2 nm. The average spectrum from two measurements was reported.

### 2.6. Confocal imaging

Amylin samples for confocal microscopy were prepared by ageing 25  $\mu$ M of amylin in 20 mM, pH 7.5 phosphate buffer at room temperature for 2 days, followed by TCEP (1 mM) treatment for 30 min. FLAsH (100  $\mu$ M) was added to the pre-treated amylin solution and incubated for 24 h at room temperature. Then the solution was drop-casted, mounted with FluorSave™ Reagent (Calbiochem), and left to dry on the glass slide prior to imaging. Confocal imaging was carried out with a Leica SP5 inverted confocal microscope using a 100 $\times$ 1.4 NA oil immersion objective. The laser wavelength excitation and emission filters for FLAsH were 488 nm and 503–555 nm respectively. For post-processing of the images, 16-bit raw confocal image stacks were deconvolved using Huygens Deconvolution software (Scientific Volume Image), and a confocal z-stack montage was created from the 3D data sets using ImageJ.

### 2.7. Native polyacrylamide gel electrophoresis (PAGE)

Native gel electrophoresis were performed using amylin samples that contained 0.43 mM of amylin, 1 mM TCEP and different concentrations of FLAsH (0.22 mM, 0.43 mM, and 0.86 mM) in phosphate buffer (20 mM, pH 7.5). Amylin fibrils were prepared by ageing the amylin solution (0.5 mM) for at least 24 h in the phosphate buffer (20 mM, pH 7.5). To run a native PAGE, the samples were mixed with native sample buffer (Bio-Rad), and electrophoresed in 4–20% Mini-PROTEAN® TGX™ Precast Protein Gels (Bio-Rad) in Tris-Glycine running buffer (Bio-Rad) at 80 V for 1.5 h at room temperature. The result was visualised with a BioSpectrum Imaging System (UVP) with VisionWorks LS Software (UVP) and the molecular weights were approximated using Precision Plus Protein™ Kaleidoscope™ Standards (Bio-Rad).

### 2.8. ThT assay

ThT assay was performed in a 384-well plate with a total volume of 80  $\mu$ L. The amylin solution was prepared at a concentration of 31.25  $\mu$ M in phosphate buffer (20 mM, pH 7.5), and diluted to final concentrations of 25, 20, 10, and 5  $\mu$ M with buffer. Then, 8  $\mu$ L of ThT stock solution (100  $\mu$ M) was added to the peptide solution. Fluorescence kinetics were measured on Perkin Elmer EnSpire plate reader, with a time interval of 2 min. The excitation wavelength of ThT fluorescence was 440 nm, and the emission wavelength was 485 nm. The lag time ( $t_{lag}$ ) and the time at half fluorescence maximum ( $t_{1/2}$ )

were calculated according to the method reported by Arosio and colleagues [29]. For the measurement of fibrillation kinetics in the presence of glycosaminoglycans (GAGs), 8  $\mu$ L of GAG solution (0.5 mg/mL in deionised water) were added to the amylin (10  $\mu$ M) solution, and ThT (10  $\mu$ M) was immediately added to the amylin/GAG solution prior to fluorescence measurement.

### 2.9. FLAsH binding assay

FLAsH assay was performed in a 384-well plate with a total volume of 80  $\mu$ L. The amylin solution was prepared at a concentration of 25  $\mu$ M in phosphate buffer (20 mM, pH 7.5). To reduce the disulphide bond, TCEP (1 mM) was added to the solution and left undisturbed for 15 min at room temperature. Final concentrations of 15, 12, 9, 6, and 3  $\mu$ M of TCEP-treated amylin were prepared in buffer, followed by the addition of 8  $\mu$ L of FLAsH solution (30  $\mu$ M) to the peptide solution. Fluorescence kinetics were measured on Perkin Elmer EnSpire plate reader, with a time interval of 2 min. The excitation wavelength of FLAsH fluorescence was 480 nm, and the emission wavelength was 535 nm.

### 2.10. Study of amyloid modulator/inhibitor with FLAsH assay

To screen the effect of GAGs on amylin fibrillation, 8  $\mu$ L of GAG solutions (0.5 mg/mL in deionized water) were added to the TCEP-treated amylin (10  $\mu$ M) solution, followed by the addition of FLAsH (3  $\mu$ M). The solution was left undisturbed in the dark for 2.5 h prior to fluorescence spectra measurement (Ex=480 nm, Em=490–650 nm). The inhibiting effects of epigallocatechin-3-gallate (EGCG) were demonstrated by adding the inhibitor solutions at different concentrations to the TCEP-treated amylin (10  $\mu$ M) solution, followed by the addition of FLAsH (3  $\mu$ M). The solution was left undisturbed in the dark for 1.5 h prior to fluorescence spectra measurements. The results were plotted by recording the maximum (528 nm) of each spectrum.

## 3. Results and discussion

### 3.1. Binding of FLAsH to amylin

As shown in Scheme 1, the aggregation of amylin results in the formation of a non-contiguous tetracysteine motif that can be recognised by FLAsH after cleaving the disulphide bond with tris(2-carboxyethyl)phosphine (TCEP) to produce reduced cysteines. In this process, complexation of the tetracysteine moieties and FLAsH resulted in increased fluorescence. The fibrillation of amylin is known to be accompanied by the formation of  $\beta$ -sheets, driven by multiple hydrogen bonding and hydrophobic interactions between amyloid sequences (residues 20–29). CD spectra confirmed a conformational change of amylin from random coils into extensive  $\beta$ -sheets in aqueous solution

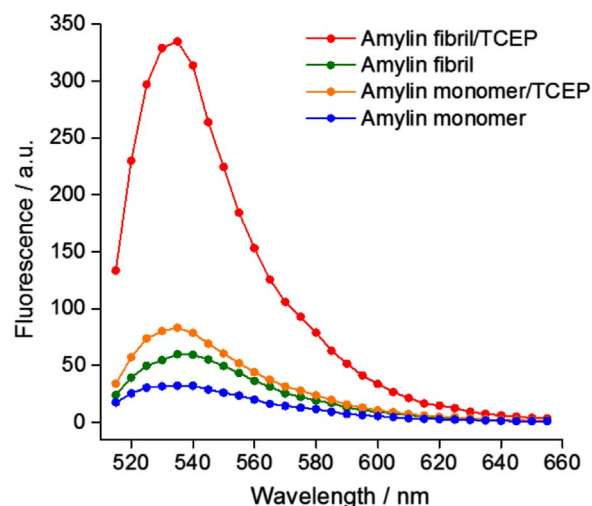


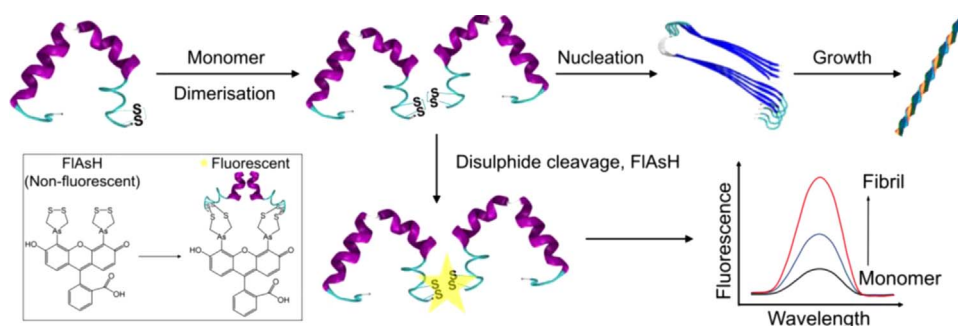
**Fig. 1.** Fluorescence spectra of FLAsH (1  $\mu$ M) in the presence of amylin (10  $\mu$ M) monomers and fibrils, and with or without cysteine reduction by TCEP (1 mM).

(Fig. S1), where the non-aggregated amylin showed a signal at 202 nm, and the mature fibril showed a peak at 218 nm due to the existence of  $\beta$ -sheets.

Amylin fibrillation was known to be governed by the core amyloidogenic sequence at the C-terminal domain (amylin residues 20–29) [30,31]. Since the binding site of FLAsH to amylin was located at the N-terminal domain, which is not responsible for protein self-assembly [32,33], the addition of FLAsH was not supposed to induce aggregation of amylin. Actually, the fibrillation kinetics were not noticeably altered after cysteine reduction (Fig. S2). This also agrees with the previous study by Lee et al. [27], in which FLAsH did not alter the amyloid fibrillation pathway of cysteine-modified A $\beta$ . The effective binding of FLAsH to reduced-cysteine amylin was further demonstrated by fluorescence spectroscopy with a five-fold increase in fluorescence intensity being observed for amylin in its fibrillar state compared to the monomeric form (Fig. 1). In addition, FLAsH exhibited low fluorescence in both monomeric and fibrillar amylin samples in the absence of TCEP, indicating that the cleavage of disulphides was crucial for the detection of intermolecular protein assembly.

### 3.2. Imaging of amylin fibrils with FLAsH

Amylin fibrillation was further confirmed by transmission electron microscopy (TEM) and atomic force microscopy (AFM), showing mature amylin fibrils had an average height of 5 nm, width of 10 nm and length of several hundred nanometres (Fig. 2a, S3). Here, the five-fold fluorescence enhancement of FLAsH upon reacting with aggregated amylin (Fig. 1) has enabled us to image the amylin fibrils with good



**Scheme 1.** Schematic view of the detection of amylin nucleation by FLAsH. The mechanism of amyloid fibrillation involves multiple processes, in which protein oligomers transform first into protofibrils and then further grow into amyloid fibrils. FLAsH can react with dimerised amylin through four reduced thiol groups in close proximity, formed by cleaving the intrinsic disulphide bonds at the N-terminal region by TCEP. The inset figure shows the “turn-on” fluorescence by the tetracysteine recognition by cleaving the intrinsic disulphide bonds at the N-terminal region by TCEP.



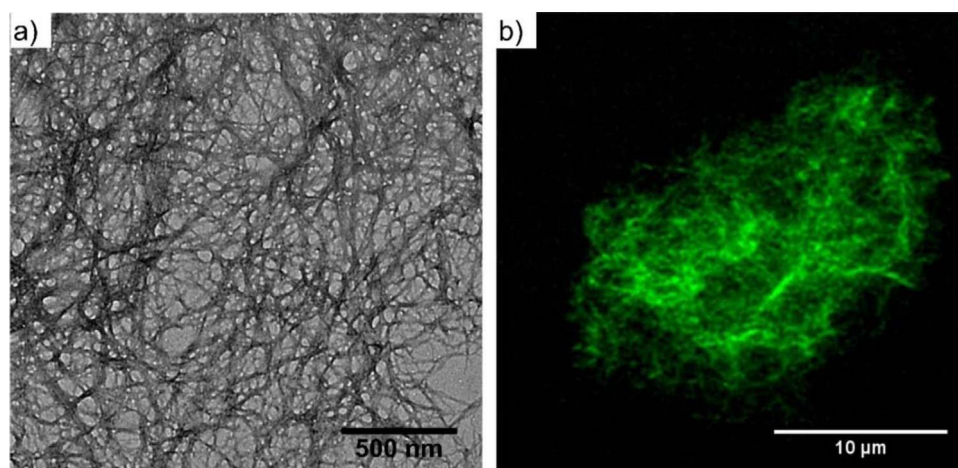


**Fig. 2.** Imaging of amylin fibrils by (a) TEM and (b) confocal microscopy. In (b), the fibrillar structures with green fluorescence supports the binding of FAsH to amylin.

signal-to-noise ratio by confocal microscopy, which could be considered as a complementary technique for imaging of amyloid fibrils. As shown in Fig. 2b, S4 and Video S1, FAsH-labelled amylin fibrils further aggregated into a 3D network, which displayed an average thickness of  $5.20 \pm 1.18 \mu\text{m}$  along the axis of the imaging sections. The co-localisation of individual amylin fibrils and FAsH fluorescence confirmed the fluorescence enhancement was due to FAsH-amylin complexation. As shown in Fig. S5, a bonus for FAsH labelling was that the arsenic ligand did not interact with reduced glutathione (GSH,

10 mM), which is commonly presented in living cells at a millimolar concentration [34,35].

Supplementary material related to this article can be found online at <http://dx.doi.org/10.1016/j.talanta.2017.05.015>.

### 3.3. Early detection of amylin fibrillation with FAsH

ThT kinetic assay is the typical method that has been established to study the self-assembly of amyloid proteins. However, the ThT assay is

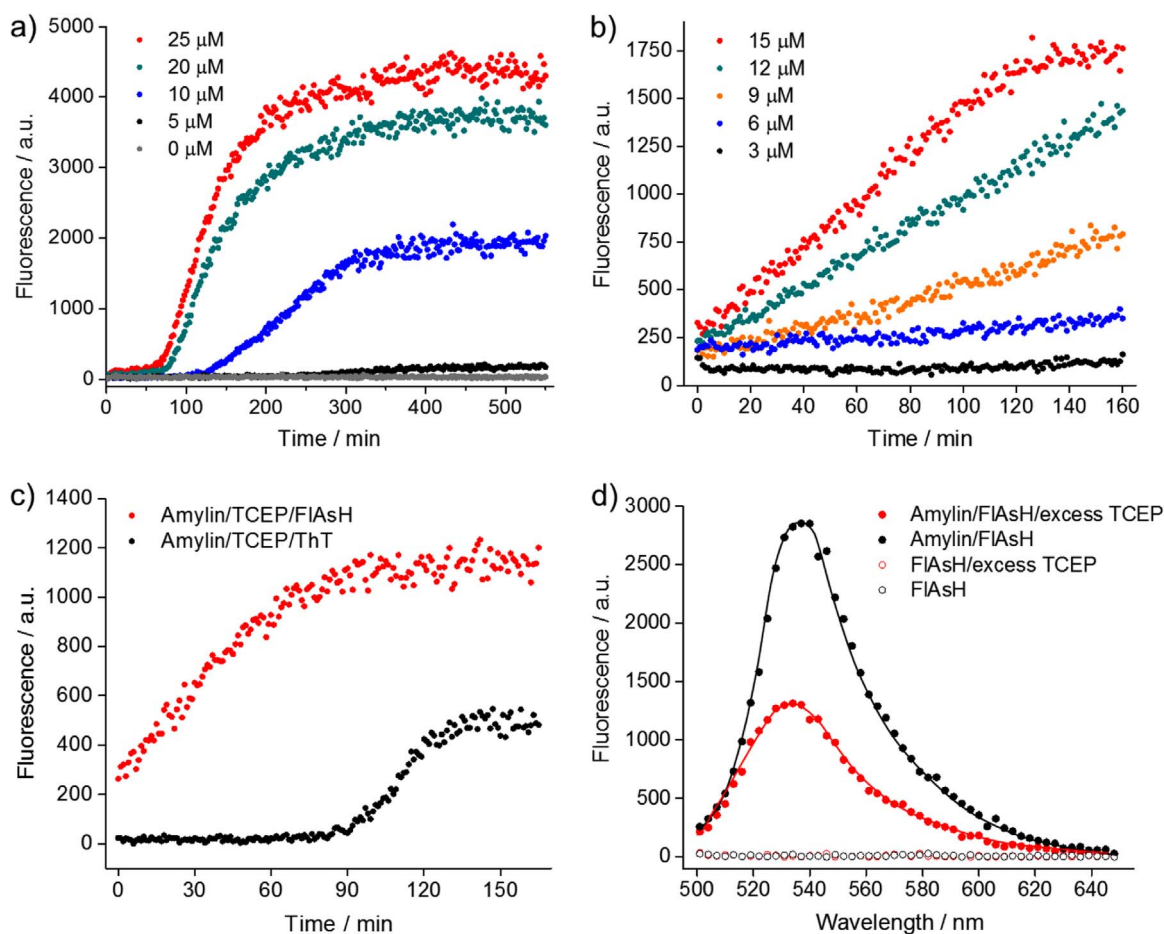


**Fig. 3.** Comparison of FAsH and ThT assays in the detection of amylin fibrillation. (a) ThT and (b) FAsH assay monitoring the amylin fibrillation kinetics. (c) Kinetic assay of amylin (10  $\mu\text{M}$ ) fibrillation with FAsH (1  $\mu\text{M}$ ) and ThT (1  $\mu\text{M}$ ), showing the early-detection of amylin nucleation with FAsH. (d) Fluorescence spectra of FAsH in amylin solutions (20  $\mu\text{M}$ ) with and without excess TCEP (50 mM).

not able to detect oligomer formation at the early stage of protein fibrillation. As shown in Fig. 3a, the kinetics of amylin self-assembly displayed a sigmoidal shape, in which the nucleation phase (or lag phase) showed low fluorescence and was followed by a transition zone (the growth phase) that exhibited an exponential increase in the emission intensity. At the final stage, the maximised and stabilised fluorescence emission represented a steady state where the fibril concentration reached its equilibrium value. The fibrillation kinetics were dependent on the protein concentration, which could be determined by fitting the sigmoidal curves to extrapolate the lag time ( $t_{lag}$ , the duration of lag phase), and the half time ( $t_{1/2}$ , the amplitude of nucleation-growth transition) (Fig. S6). As shown in Fig. S6a,  $t_{lag}$  at low emission intensity was calculated to be within 1–3.5 h depending on the amylin concentration between 5–25  $\mu\text{M}$ .

Unlike the ThT assay, amylin fibrillation reported by FLAsH fluorescence showed a rapid increase in emission intensity, with the fluorescence enhancement being correlated with protein concentration (Fig. 3b). As shown in Fig. S7, a linear correlation between the increasing rate of fluorescence intensity and protein concentration was found. This suggests that molecular association between two amylin proteins could rapidly form oligomeric intermediates, which served as nucleation seeds for fibril growth and elongation [36–38]. Native polyacrylamide gel electrophoresis (PAGE) showed the formation of amylin oligomers (~10 kDa) that could be detected by FLAsH (Fig. S8). Amylin aggregation into large fibrils could be confirmed by the 1.2 times enhanced fluorescence intensities of the freshly prepared amylin solution, compared to the fibril samples.

The advantages of FLAsH over ThT in monitoring the initial events of amylin fibrillation were further demonstrated when the fluorescence emission of 1  $\mu\text{M}$  of FLAsH ( $E_x=480$  nm and  $E_m=535$  nm) and ThT ( $E_x=440$  nm and  $E_m=485$  nm) were simultaneously recorded in the presence of 10  $\mu\text{M}$  amylin. It is noted that the FLAsH fluorescence reaching its maximum at 1.5 h preceded the ThT-monitored growth phase associated with amyloid fibril formation (Fig. 3c). This phenomenon is likely to originate from the different fluorescence emission mechanisms of FLAsH and ThT, where ThT specifically targets  $\beta$ -sheet structures, while FLAsH can recognise the formation of dimers and oligomers at the early stage. Moreover, addition of excess TCEP (50 mM) to the amylin/FLAsH conjugates showed a reduction in the fluorescence intensity (Fig. 3d), indicating that enhanced fluorescence originated from covalent bonding between FLAsH and amylin.

### 3.4. Examination of amyloid inhibitor and modulator with FLAsH

We applied the FLAsH assay to examine amylin fibrillation in the presence of amyloid inhibitors and modulators. It is known that

polyphenol derivatives such as epigallocatechin-3-gallate (EGCG) can redirect the amyloid aggregation pathway and inhibit the fibril formation [39–41]. Indeed, the inhibition effect of EGCG (50  $\mu\text{M}$ ) towards amylin aggregation was observed from the decrease of FLAsH fluorescence in a concentration-dependent manner (Fig. 4). By fitting the concentration-fluorescence curve, the  $IC_{50}$  of EGCG was determined to be 0.3  $\mu\text{M}$  (Fig. 4b).

The FLAsH assay was also applied to screen the effect of GAG-based amyloid modulators. GAGs are a subfamily of carbohydrate polymers that function in various biological processes, with changes in the chemical structure (*e.g.* charge, acetylation, and sulphonation) significantly affecting biological activity. Among the macromolecules, those containing strong negative charge lead to a strong affinity for amyloid precursors and promote nucleation into fibrils [42]. In particular, sulphated GAGs, which are abundant components of the extracellular matrix of many tissues, have been reported to stabilise the mature fibrils and prevent dissociation and proteolytic degradation [43–45]. To distinguish the differences between GAGs in regulating amylin self-assembly, we compared the enhanced FLAsH fluorescence in amylin solutions in the presence of five selected GAGs, dextran sulphate (G1), heparin sulphate (G2), N-acetyl-de-O-sulphated heparin sodium salt (G3), hyaluronic acid sodium salt (G4), and chitosan (G5). We found that G1 and G2 showed the highest effect in promoting amylin aggregation as the strongest fluorescence was noted in both cases. Control experiments showed the fluorescence increase was not due to GAG/FLAsH interactions since GAGs themselves did not cause enhanced emission (Fig. 5a).

In contrast, G3, G4 and G5 did not noticeably affect the self-assembly of amylin at the same concentration. To interpret this result, it is necessary to consider the molecular structure of the GAGs. As shown in Fig. 5b, the GAGs consist of disaccharide repeating units with different anionic groups (*i.e.*, carboxyl, and sulphate groups, except for chitosan) on the backbones [46]. Considering the possession of four positive charges on amylin, it is reasonable that electrostatic attractions may dominate the GAG/amylin interactions. In the literature, charge interactions between nanoparticles and amyloid proteins have been shown to accelerate the fibrillation process due to the generation of localised nucleation sites, causing the enhanced propagation into fibrils [47,48]. Here, G1 and G2 possess four negative charges on each disaccharide unit and could complex with the positively-charged amylin more effectively than G3, G4, and G5 (which have two, one, and no charges, respectively), and result in a higher fibrillation rate. This finding was consistent with the ThT assay (Fig. S9), where a significant increase in fluorescence was also observed in the presence of G1 and G2 after 2.5 h, while the other GAG modulators showed less

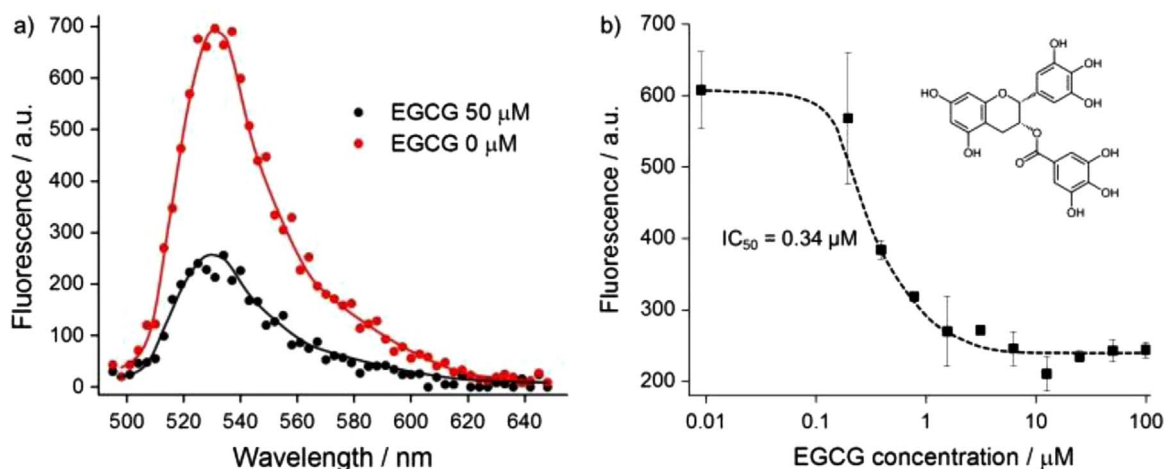


**Fig. 4.** Inhibition of amylin self-association by EGCG studied by FLAsH assay. (a) Fluorescence spectra of FLAsH probe in a solution of amylin (10  $\mu\text{M}$ ) in the presence and absence of EGCG. The amylin/EGCG mixtures were incubated for 1.5 h before the fluorescence measured. (b) Fluorescence intensity of FLAsH probe ( $E_x=480$  nm,  $E_m=528$  nm) in a solution of amylin (10  $\mu\text{M}$ ) containing different concentrations of EGCG. The inset figure shows the molecular structure of EGCG.

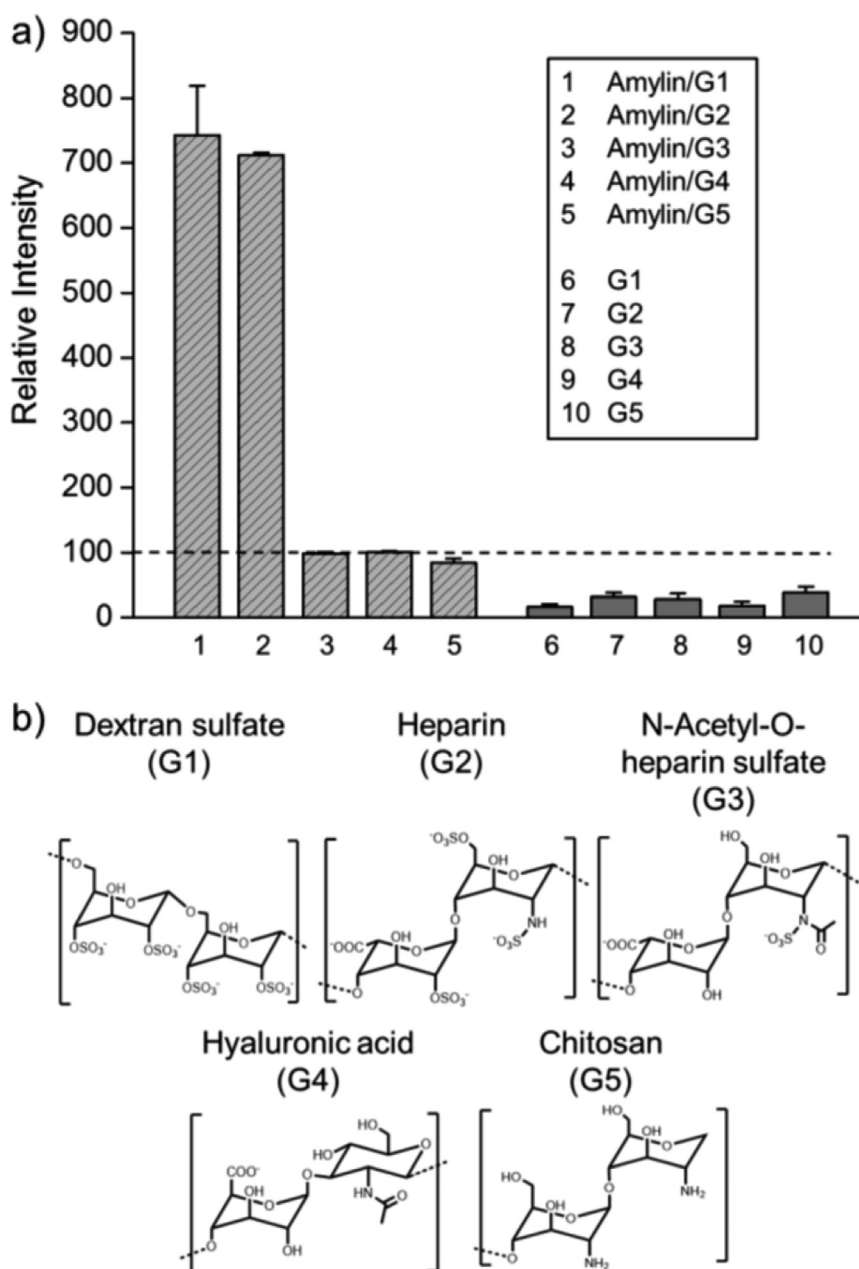


**Fig. 5.** Effect of GAGs on the degree of amylin self-association via FLAsH assay. (a) Fluorescence intensity of FLAsH probe in a solution of amylin in the presence of GAGs (Ex=480 nm, Em=528 nm). The amylin/GAG mixtures were incubated for 2.5 h before the fluorescence intensity was measured, and the intensities were calculated relative to a control sample in the absence of GAG. (b) Molecular structure of the GAGs (G1: dextran sulphate, G2: heparin sulphate, G3: N-acetyl-de-O-sulphated heparin sodium salt, G4: hyaluronic acid sodium salt, G5: chitosan).

effect on amylin fibrillation (Fig. S9b). It is noted that the background of FLAsH fluorescence in the GAG solutions was negligible since there were not tetracysteine motifs or free thiols present in the backbone of GAGs. In contrast, ThT fluorescence in GAG solutions showed varied fluorescence background possibly due to the fact that rigid polysaccharide backbones can restrict the rotational motion of ThT and enhance its fluorescence quantum yield. We anticipate that the FLAsH assay developed here will be applicable to the discrimination of natural amyloid modulators, and high-throughput screening of small molecule inhibitors for amylin fibrillation.

#### 4. Conclusions

In conclusion, we have developed a new strategy to detect amylin fibrillation at an early stage using a tetracysteine-binding FLAsH dye.

This method specifically recognised the intrinsic disulphide bonds on two adjacent amylin motifs. Importantly, the assay detected the native structure without causing perturbation of the aggregation pathway. The *in situ* efficient conjugation of FLAsH to associated amylin in the fibrillar form enabled the fluorescence imaging of the amyloid fibrils. Since FLAsH is known to have cell permeability [24,49], it is expected that this method can allow localised cellular imaging of the aggregated proteins. Compared to the commonly used ThT fluorescence assay, this method notably allowed concentration-dependent kinetics studies of the early nucleation events, which are key features in the aggregation mechanism of many proteins. The FLAsH assay was also able to monitor the extent of fibrillation in the presence of amylin inhibitors and modulators. This approach applying a concentration-dependent study, specifically recognising amino acid residues of the native protein structure, is expected to be useful for further investigations into the



mechanistic details controlling self-assembly in other aggregation-prone proteins.

## Acknowledgements

S.-T.W. and C.-C.H. thank the support of the Top University Strategic Alliance Ph.D. scholarship from Taiwan. N.A. was supported by Marie Curie actions FP7 through the Intra-European Marie Curie Fellowship “ConPilus” under grant agreement no. 623123. C.D.S. and M.M.S. acknowledge the Engineering and Physical Sciences Research Council (EPSRC) grant “Bio-functionalised nanomaterials for ultra-sensitive biosensing” (EP/K020641/1). M.M.S. also acknowledges support from the ERC Seventh Framework Programme Consolidator grant “Naturale CG” under Grant Agreement No. 616417 and the EPSRC Interdisciplinary Research Centre (IRC) “Early-Warning Sensing Systems for Infectious Diseases” (EP/K031953/1). Raw data is available online at <http://dx.doi.org/10.5281/zenodo.259524>.

## Appendix A. Supplementary material

Supplementary data associated with this article can be found in the online version at <http://dx.doi.org/10.1016/j.talanta.2017.05.015>.

## References

- [1] J.M. Forbes, M.E. Cooper, Mechanisms of diabetic complications, *Physiol. Rev.* 93 (1) (2013) 137–188.
- [2] J.W.M. Höppener, B. Ahren, C.J.M. Lips, Islet amyloid and type 2 diabetes mellitus, *N. Engl. J. Med.* 343 (6) (2000) 411–419.
- [3] G.M. Shankar, S. Li, T.H. Mehta, A. Garcia-Munoz, N.E. Shepardson, I. Smith, F.M. Brett, M.A. Farrell, M.J. Rowan, C.A. Lemere, C.M. Regan, D.M. Walsh, B.L. Sabatini, D.J. Selkoe, Amyloid- $\beta$  protein dimers isolated directly from Alzheimer's brains impair synaptic plasticity and memory, *Nat. Med.* 14 (8) (2008) 837–842.
- [4] R. Kaye, E. Head, J.L. Thompson, T.M. McIntire, S.C. Milton, C.W. Cotman, C.G. Glabe, Common structure of soluble amyloid oligomers implies common mechanism of pathogenesis, *Science* 300 (5618) (2003) 486–489.
- [5] M. Fändrich, Oligomeric intermediates in amyloid formation: structure determination and mechanisms of toxicity, *J. Mol. Biol.* 421 (4–5) (2012) 427–440.
- [6] D. Zanuy, B. Ma, R. Nussinov, Short peptide amyloid organization: stabilities and conformations of the islet amyloid peptide NFGAIL, *Biophys. J.* 84 (3) (2003) 1884–1894.
- [7] S.L. Bernstein, N.F. Dupuis, N.D. Lazo, T. Wytenbach, M.M. Condron, G. Bitan, D.B. Teplow, J.-E. Shea, B.T. Ruotolo, C.V. Robinson, M.T. Bowers, Amyloid- $\beta$  protein oligomerization and the importance of tetramers and dodecamers in the aetiology of Alzheimer's disease, *Nat. Chem.* 1 (4) (2009) 326–331.
- [8] L. Wei, P. Jiang, W. Xu, H. Li, H. Zhang, L. Yan, M.B. Chan-Park, X.-W. Liu, K. Tang, Y. Mu, K. Pervushin, The molecular basis of distinct aggregation pathways of islet amyloid polypeptide, *J. Biol. Chem.* 286 (8) (2011) 6291–6300.
- [9] G. Bitan, M.D. Kirkitadze, A. Lomakin, S.S. Vollers, G.B. Benedek, D.B. Teplow, Amyloid  $\beta$ -protein (A $\beta$ ) assembly: A $\beta$ 40 and A $\beta$ 42 oligomerize through distinct pathways, *Proc. Natl. Acad. Sci. USA* 100 (1) (2003) 330–335.
- [10] Y.-R. Chen, C.G. Glabe, Distinct early folding and aggregation properties of Alzheimer amyloid- $\beta$  peptides A $\beta$ 40 and A $\beta$ 42: stable trimer or tetramer formation by A $\beta$ 42, *J. Biol. Chem.* 281 (34) (2006) 24414–24422.
- [11] W. Hwang, S. Zhang, R.D. Kamm, M. Karplus, Kinetic control of dimer structure formation in amyloid fibrillogenesis, *Proc. Natl. Acad. Sci. USA* 101 (35) (2004) 12916–12921.
- [12] L. Yu, R. Edalji, J.E. Harlan, T.F. Holzman, A.P. Lopez, B. Labkovsky, H. Hillen, S. Barghorn, U. Ebert, P.L. Richardson, L. Miesbauer, L. Solomon, D. Bartley, K. Walter, R.W. Johnson, P.J. Hajduk, E.T. Olejniczak, Structural characterization of a soluble amyloid  $\beta$ -peptide oligomer, *Biochemistry* 48 (9) (2009) 1870–1877.
- [13] C.G. Glabe, Structural classification of toxic amyloid oligomers, *J. Biol. Chem.* 283 (44) (2008) 29639–29643.
- [14] M. Ahmed, J. Davis, D. Aucoin, T. Sato, S. Ahuja, S. Aimoto, J.I. Elliott, W.E. Van Nostrand, S.O. Smith, Structural conversion of neurotoxic amyloid- $\beta$ 1–42 oligomers to fibrils, *Nat. Struct. Mol. Biol.* 17 (5) (2010) 561–567.
- [15] T.H.J. Huang, D.-S. Yang, N.P. Plaskos, S. Go, C.M. Yip, P.E. Fraser, A. Chakrabarty, Structural studies of soluble oligomers of the Alzheimer  $\beta$ -amyloid peptide1, *J. Mol. Biol.* 297 (1) (2000) 73–87.
- [16] G.T. Westermark, K.H. Johnson, P. Westermark, [1] Staining Methods for Identification of Amyloid in Tissue, *Methods Enzymol.* Academic Press, 1999, pp. 3–25.
- [17] R. Mishra, D. Sjolander, P. Hammarstrom, Spectroscopic characterization of diverse amyloid fibrils in vitro by the fluorescent dye Nile red, *Mol. Biosyst.* 7 (4) (2011) 1232–1240.
- [18] H. Levine, Thioflavine T interaction with synthetic Alzheimer's disease  $\beta$ -amyloid peptides: detection of amyloid aggregation in solution, *Protein Sci.* 2 (3) (1993) 404–410.
- [19] A. Hawe, M. Sutter, W. Jiskoot, Extrinsic fluorescent dyes as tools for protein characterization, *Pharm. Res.* 25 (7) (2008) 1487–1499.
- [20] Y. Bram, A. Lampel, R. Shaltiel-Karyo, A. Ezer, R. Scherzer-Attali, D. Segal, E. Gazit, Monitoring and targeting the initial dimerization stage of amyloid self-assembly, *Angew. Chem. Int. Ed.* 54 (7) (2015) 2062–2067.
- [21] T. Takahashi, H. Mihara, FRET detection of amyloid  $\beta$ -peptide oligomerization using a fluorescent protein probe presenting a pseudo-amyloid structure, *Chem. Commun.* 48 (10) (2012) 1568–1570.
- [22] N. Pradhan, D. Jana, B.K. Ghorai, N.R. Jana, Detection and monitoring of amyloid fibrillation using a fluorescence “switch-On” probe, *ACS Appl. Mater. Interfaces* 7 (46) (2015) 25813–25820.
- [23] K.L. Viola, J. Sbarboro, R. Sureka, M. De, M.A. Bicca, J. Wang, S. Vasavada, S. Satpathy, S. Wu, H. Joshi, P.T. Velasco, K. MacRenaris, E.A. Waters, C. Lu, J. Phan, P. Lacor, P. Prasad, V.P. Dravid, W.L. Klein, Towards non-invasive diagnostic imaging of early-stage Alzheimer's disease, *Nat. Nanotechnol.* 10 (1) (2015) 91–98.
- [24] S.R. Adams, R.E. Campbell, L.A. Gross, B.R. Martin, G.K. Walkup, Y. Yao, J. Llopis, R.Y. Tsien, New biarsenical ligands and tetracysteine motifs for protein labeling in vitro and in vivo: synthesis and biological applications, *J. Am. Chem. Soc.* 124 (21) (2002) 6063–6076.
- [25] B.A. Griffin, S.R. Adams, R.Y. Tsien, Specific covalent labeling of recombinant protein molecules inside live cells, *Science* 281 (5374) (1998) 269–272.
- [26] N.W. Luedtke, R.J. Dexter, D.B. Fried, A. Schepartz, Surveying polypeptide and protein domain conformation and association with FLaSh and ReAsH, *Nat. Chem. Biol.* 3 (12) (2007) 779–784.
- [27] J. Lee, E.K. Culyba, E.T. Powers, J.W. Kelly, Amyloid- $\beta$  forms fibrils by nucleated conformational conversion of oligomers, *Nat. Chem. Biol.* 7 (9) (2011) 602–609.
- [28] O. Sumner Makin, L.C. Serpell, Structural characterisation of islet amyloid polypeptide fibrils, *J. Mol. Biol.* 335 (5) (2004) 1279–1288.
- [29] P. Arosio, T.P.J. Knowles, S. Linse, On the lag phase in amyloid fibril formation, *Phys. Chem. Chem. Phys.* 17 (12) (2015) 7606–7618.
- [30] T.T. Ashburn, P.T. Lansbury, Interspecies sequence variations affect the kinetics and thermodynamics of amyloid formation: peptide models of pancreatic amyloid, *J. Am. Chem. Soc.* 115 (23) (1993) 11012–11013.
- [31] P. Westermark, U. Engstrom, K.H. Johnson, G.T. Westermark, C. Betsholtz, Islet amyloid polypeptide: pinpointing amino acid residues linked to amyloid fibril formation, *Proc. Natl. Acad. Sci. USA* 87 (13) (1990) 5036–5040.
- [32] J.R. Brender, E.L. Lee, M.A. Cavitt, A. Gafni, D.G. Steel, A. Ramamoorthy, Amyloid fiber formation and membrane disruption are separate processes localized in two distinct regions of IAPP, the type-2-diabetes-related peptide, *J. Am. Chem. Soc.* 130 (20) (2008) 6424–6429.
- [33] D.H. Lopes, A. Meister, A. Gohlke, A. Hauser, A. Blume, R. Winter, Mechanism of islet amyloid polypeptide fibrillation at lipid interfaces studied by infrared reflection absorption spectroscopy, *Biophys. J.* 93 (9) (2007) 3132–3141.
- [34] A. Meister, M.E. Anderson, Glutathione, *Annu. Rev. Biochem.* 52 (1) (1983) 711–760.
- [35] A. Pastore, G. Federici, E. Bertini, F. Piemonte, Analysis of glutathione: implication in redox and detoxification, *Clin. Chim. Acta* 333 (1) (2003) 19–39.
- [36] M.M. Pallitto, R.M. Murphy, A mathematical model of the kinetics of beta-amyloid fibril growth from the denatured state, *Biophys. J.* 81 (3) (2001) 1805–1822.
- [37] V.N. Uversky, A.L. Fink, Conformational constraints for amyloid fibrillation: the importance of being unfolded, *Biochim. Biophys. Acta* 1698 (2) (2004) 131–153.
- [38] Y. Liang, D.G. Lynn, K.M. Berland, Direct observation of nucleation and growth in amyloid self-assembly, *J. Am. Chem. Soc.* 132 (18) (2010) 6306–6308.
- [39] D.E. Ehrnhofer, J. Bieschke, A. Boeddrich, M. Herbst, L. Masino, R. Lurz, S. Engemann, A. Pastore, E.E. Wanker, ECGG redirects amyloidogenic polypeptides into unstructured, off-pathway oligomers, *Nat. Struct. Mol. Biol.* 15 (6) (2008) 558–566.
- [40] F. Meng, A. Abedini, A. Plesner, C.B. Verchere, D.P. Raleigh, The flavanol (-)-epigallocatechin 3-gallate inhibits amyloid formation by islet amyloid polypeptide, disaggregates amyloid fibrils, and protects cultured cells against IAPP-induced toxicity, *Biochemistry* 49 (37) (2010) 8127–8133.
- [41] P. Cao, D.P. Raleigh, Analysis of the inhibition and remodeling of islet amyloid polypeptide amyloid fibers by flavanols, *Biochemistry* 51 (13) (2012) 2670–2683.
- [42] J.Y. Suk, F. Zhang, W.E. Balch, R.J. Linhardt, J.W. Kelly, Heparin accelerates gelsolin amyloidogenesis, *Biochemistry* 45 (7) (2006) 2234–2242.
- [43] C.I. Gama, S.E. Tully, N. Sotogaku, P.M. Clark, M. Rawat, N. Vaidehi, W.A. Goddard, A. Nishi, L.C. Hsieh-Wilson, Sulfation patterns of glycosaminoglycans encode molecular recognition and activity, *Nat. Chem. Biol.* 2 (9) (2006) 467–473.
- [44] I. Yamaguchi, H. Suda, N. Tsuzuki, K. Seto, M. Seki, Y. Yamaguchi, K. Hasegawa, N. Takahashi, S. Yamamoto, F. Gejyo, H. Naiki, Glycosaminoglycan and proteoglycan inhibit the depolymerization of  $\beta$ 2-microglobulin amyloid fibrils in vitro, *Kidney Int.* 64 (3) (2003) 1080–1088.
- [45] R. Gupta-Bansal, R.C.A. Frederickson, K.R. Brunden, Proteoglycan-mediated inhibition of A $\beta$  proteolysis: a potential cause of senile plaque accumulation, *J. Biol. Chem.* 270 (31) (1995) 18666–18671.
- [46] Y. Lin, R. Chapman, M.M. Stevens, Integrative self-assembly of graphene quantum dots and biopolymers into a versatile biosensing Toolkit, *Adv. Funct. Mater.* 25 (21) (2015) 3183–3192.
- [47] Y. Kim, J.-H. Park, H. Lee, J.-M. Nam, How do the size, charge and shape of nanoparticles affect amyloid  $\beta$  aggregation on brain lipid bilayer?, *Sci. Rep.* 6 (2016) 19548.
- [48] S. Linse, C. Cabaleiro-Lago, W.-F. Xue, I. Lynch, S. Lindman, E. Thulin, S.E. Radford, K.A. Dawson, Nucleation of protein fibrillation by nanoparticles, *Proc. Natl. Acad. Sci. USA* 104 (21) (2007) 8691–8696.
- [49] M.J. Roberti, C.W. Bertoncini, R. Klement, E.A. Jares-Erijman, T.M. Jovin, Fluorescence imaging of amyloid formation in living cells by a functional, tetracysteine-tagged alpha-synuclein, *Nat. Methods* 4 (4) (2007) 345–351.